Electronic Supplementary Material (ESI) for Green Chemistry.

SUPPORTING INFORMATION

Hybrid Wood Materials with Improved Fire Retardance by Bio-inspired Mineralization on Nano- and Submicron Level

Vivian Merk, Munish Chanana*, Tobias Keplinger, Sabyasachi Gaan, Ingo Burgert*

Experimental section

Mineralization of wood: Blocks of Norway spruce (Picea abies) and European beech (Fagus sylvatica) (10 mm or 20 mm edge length) were conditioned at norm climate (65 % relative humidity, 20° C) and dried in a BINDER vacuum oven at 65°C for 48 h. The presented mineralization approach is a facile one-pot process in water at room temperature. Dimethyl carbonate (Sigma Aldrich Reagent Plus, 99 %), calcium chloride dihydrate (Merck, EMSURE ACS Reag. PhEur) and sodium hydroxide (pellets for analysis, Merck, ACS Reag. PhEur) were used without prior purification. Equimolar amounts of dimethyl carbonate and $CaCl_2$ (0.5 mol L^{-1}, 1.0 mol L^{-1}, 1.5 mol L^{-1}) were dissolved in deionized water at ambient temperature and stirred vigorously. The wood samples were incubated for 24 h in the saturated solutions and vacuum-impregnated for several times to allow for in-depth diffusion into the porous wood structure. After initiating the hydrolysis of the organic precursor by adding a 1 M solution of sodium hydroxide until a solution pH $\approx$ 9 was reached, the wood samples were kept for additional 24 h in the reaction solution. Upon addition of excess sodium hydroxide solution a quantitative hydrolysis of the precursor dimethyl carbonate can be achieved. Finally, the samples were washed with deionized water for 1 h and dried in oven 65°C until weight constancy, in order to remove water, the byproduct methanol (bp: 65°C) and DMC (bp: 90°C) . The mass gain of the samples was determined in the oven-dry state and under norm climate conditions before and after mineralization (see Figure S5, supporting information).

Light microscopy: Cross-cut wood specimens were observed under a Leica M165C stereomicroscope (3.2x objective) coupled to a Basler GigE Vision camera. Images were recorded with a control plugin (PHASE GmbH) for the programme ImageJ 1.47c.

Scanning electron microscopy: Environmental scanning electron microscopy (ESEM) was carried out on a FEI Quanta 600 in the low-vacuum mode (water vapour, 0.53 Torr) driven by 20 kV acceleration voltage using a spot size of 6.0 using a backscattered electron detector. Energy-dispersive X-ray analysis was performed on a FEI Quanta 200 3D scanning electron microscope in the low-vacuum mode (water vapour, 0.53 Torr) driven by 20 kV acceleration voltage using a spot size of 6.0 using a backscattered electron detector.

Raman microscopy: For the Raman measurements 20 µm cross-sections were prepared with a rotary microtome (Leica Ultracut, Germany)), placed on a microscopic slide with a few drops of methanol and sealed with a cover slip and nail polish to avoid evaporation. All Raman spectra were recorded with a confocal Raman-microscope (Renishaw InVia) equipped with a Nd-YAG laser (λ = 532 nm), a 1800 grooves/mm grating and a 100x oil immersion objective (Nikon, NA = 1.4), a step width of 300 nm and an integration time of 0.15 s (spruce) or 0.30 s (beech) due to higher fluorescence. The data were processed with the software Wire 3.4 and single spectra plotted with the program OriginPro 8.1. Additionally, for the extraction of hyperspectral data, the spectral dataset was scanned for cosmic rays and Vertex Component Analysis (VCA) was performed in the spectral range 900-1200 cm^{-1} with the MatLab-based software CytoSpec v. 2.00.01 assuming six endmembers.

Infrared spectroscopy: FT-IR spectra of chopped wood samples were collected with a Tensor 27 spectrometer (Bruker) eqipped with a Pike ATR cell in a spectral range of 4000-350 cm^{-1} with 4 cm^{-1} spectral resolution and averaged over 100 scans. The spectra were recorded and background-corrected with the program OPUS and plotted with OriginPro 8.1.

Pyrolysis combustion flow calorimetry: The heat of combustion of wood-$CaCO_3$ composites and reference wood conditioned to norm climate was determined by oxygen consumption applied to the combustion gases in pyrolysis combustion flow calorimetry (PCFC) (Fire Testing Technology Instrument UK) according to the procedure described in the literature [1] with a pyrolysis temperature of 85−750°C and a 80 % N_2/20 % O_2 gas mixture and operated at a heating rate of $\beta = 1\ K\ s^{-1}$ and a combustion temperature of 900°C. The PCFC measurements were replicated at least five times for samples of approximately 5 mg. The HRR curves were baseline-corrected and fitted with multiple Gauss curves using the program OriginPro 8.1. Herein, the resulting peak sum (the total heat release) displayed residual values close to 1. The maximum heat release divided by the constant heating rate $\beta = 1\ K\ s^{-1}$ gives the heat release capacity.

Thermogravimetric analysis: Thermogravimetric analyses of ~10 mg wood specimens were performed using a Q50 TGA (TA instruments) with a heating rate of 20° C min^{-1} in a N_2 atmosphere (60 mL min^{-1} sample purge flow, 40 mL min^{-1} balance purge flow in the 30-1000° C temperature range.

X-ray powder diffraction: XRD spectra were collected from a chopped mineralized spruce sample (~0.25 cm^3) on a Bruker D8 Advance instrument equipped with a copper X-ray source (40 kV voltage, 40 mA current) and a rotating flat disk sample holder using a scan speed of 0.15° min^{-1} in a 2θ = 10-90° range.

Characterization

Infrared spectroscopy

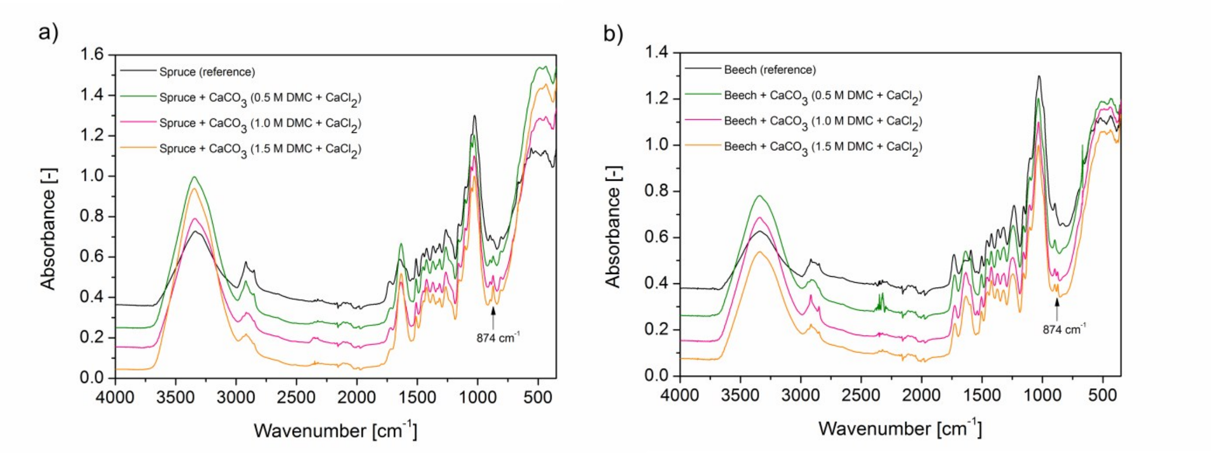

Figure S1. Typical Fourier-transform infrared spectra (FTIR) of pristine wood and CaCO$_3$/wood composites collected in the attenuated total reflection (ATR) mode: a) spruce b) beech. The ν_2 peak at 874 cm^{-1} shows the presence of calcite[2].

Raman microscopy

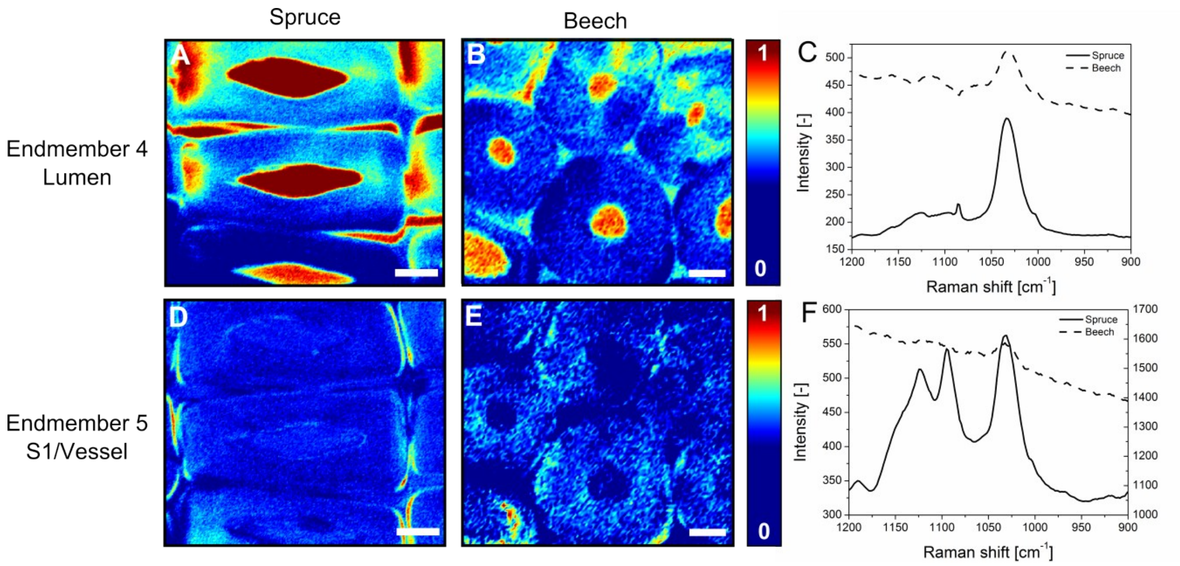

Figure S2. Raman mappings of CaCO$_3$/wood composites prepared at [DMC] = [CaCl$_2$] = 1.0 mol L^{-1} according to VCA analysis showing endmembers of spruce (A, D, solid line) and beech (B, E, dashed line) in the range |1200-900 cm^{-1}|. Endmember 4 (A, B, C): Lumen (1550-1640 cm^{-1}). Endmember 5 (D, E, F): S1 cell wall carbohydrates (1112 cm^{-1}, 1154 cm^{-1}) and beech vessel. C, F: Endmember spectra for spruce (solid line) and beech (dashed line). The left axis in F refers to spruce, the right axis to beech. Scale-bars in A and D correspond to 10 μm and in B and E to 5 μm, respectively.

Pyrolysis combustion flow calorimetry

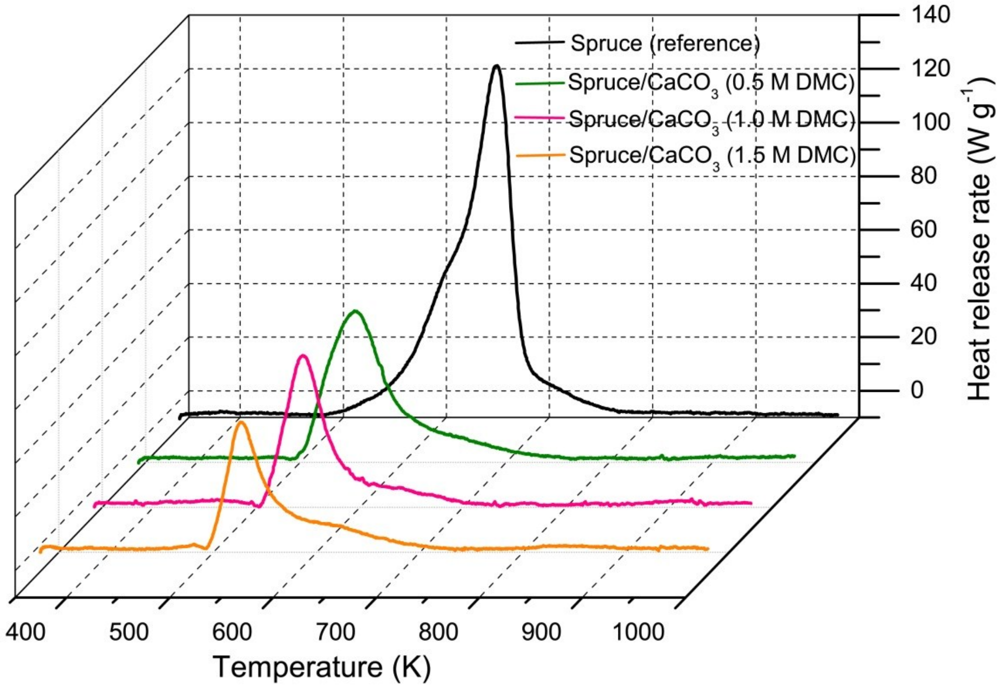

Figure S3. Pyrolysis combustion flow calorimetry: b) Typical temperature-dependent heat release rate curves of spruce samples after base-line correction.

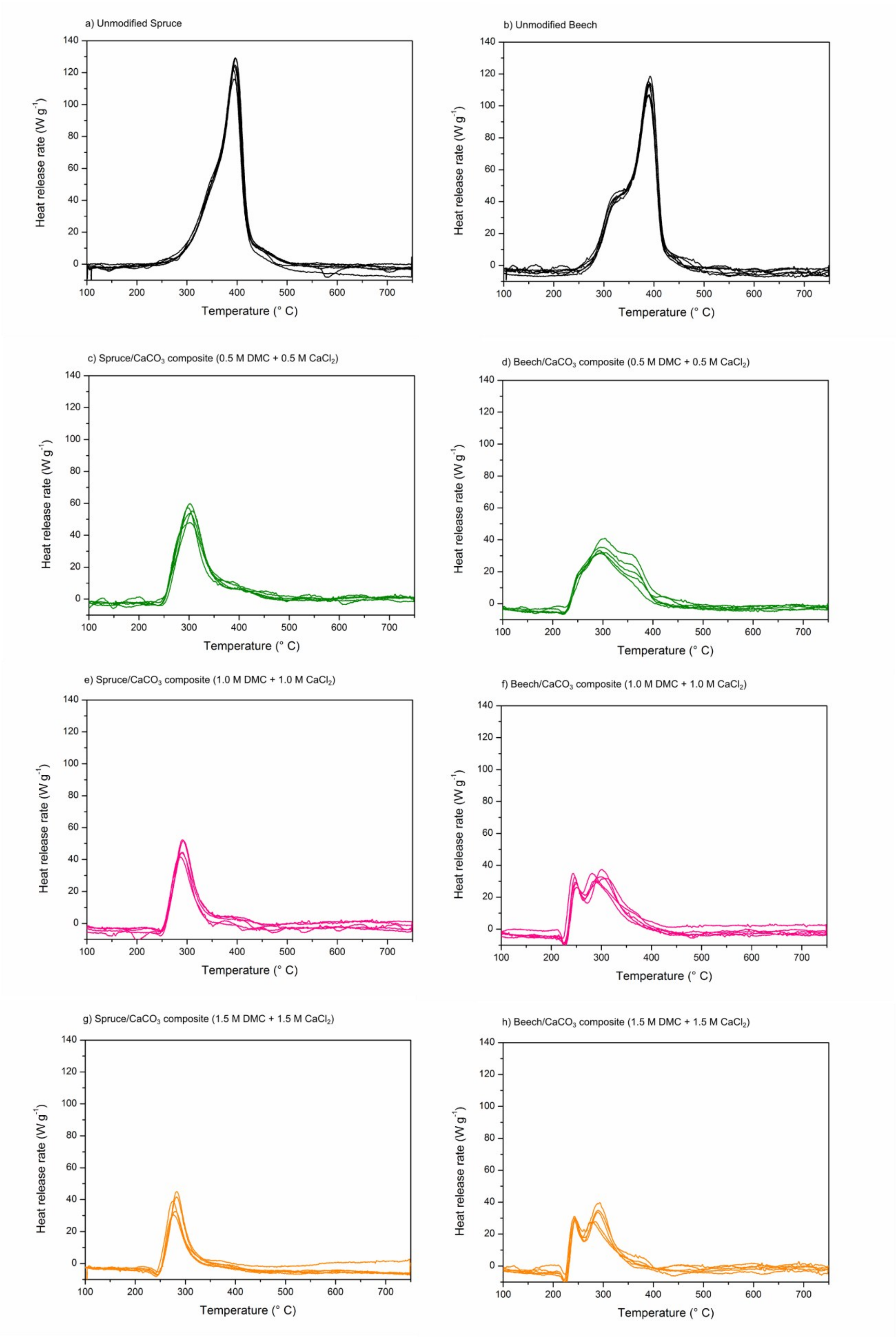

Figure S4. PCFC raw data: Temperature-dependent heat release rate curves of native wood and wood/CaCO$_3$ composites prepared from the release of CO$_2$ through a basic hydrolysis of dimethyl carbonate in the presence of calcium ions. a-d) Spruce. e-h) Beech.

Mass gain and equilibrium moisture of mineralized wood samples

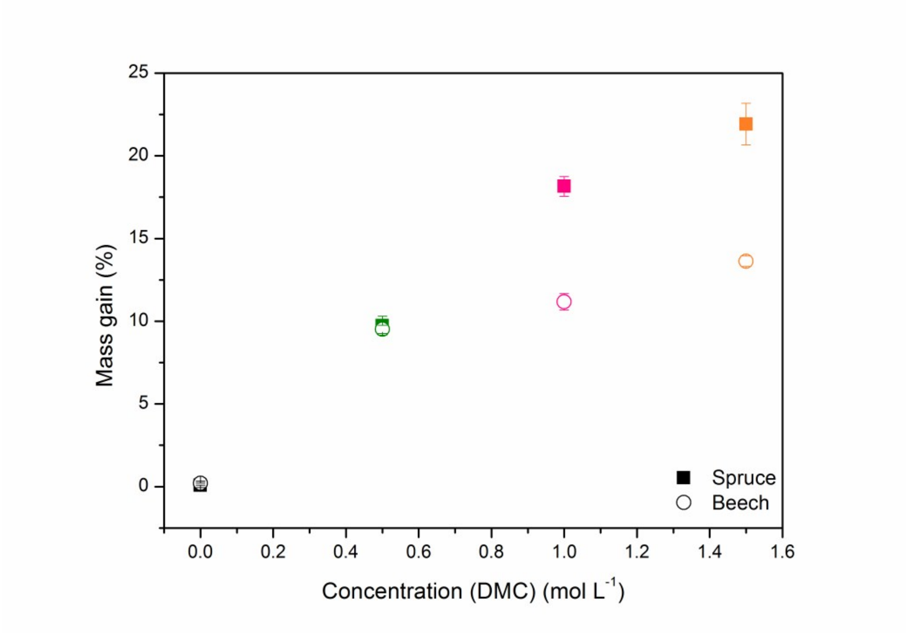

Figure S5. Mass gain of mineralized spruce and beech wood (10 mm edge length) prepared at different precursor concentrations [DMC] = [$CaCl_2$] in the dry state.

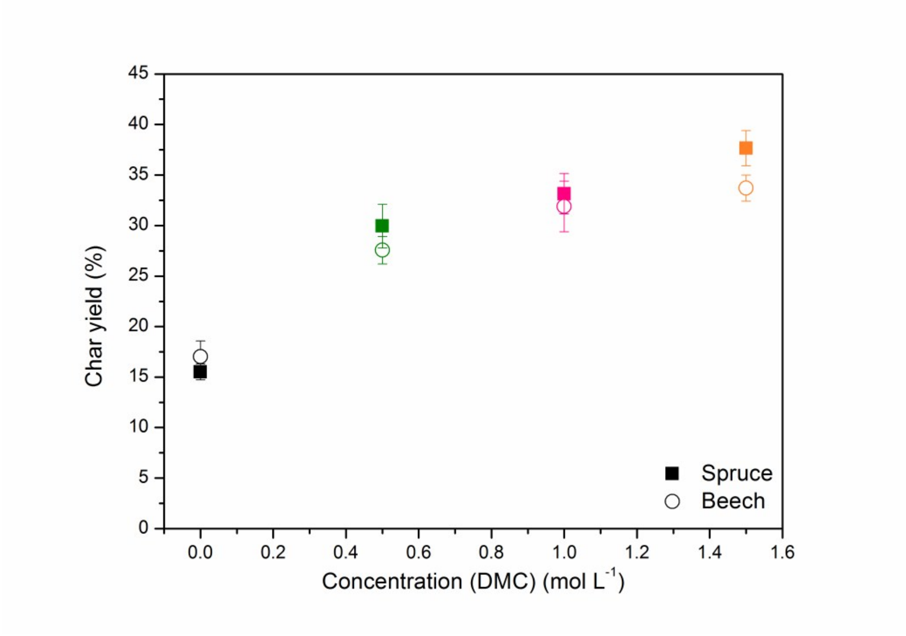

Figure S6. Char yield of native beech and spruce samples as a function of the precursor concentration [DMC] = [$CaCl_2$] calculated by weighing the test specimen before and after total combustion in pyrolysis combustion flow calorimetry.

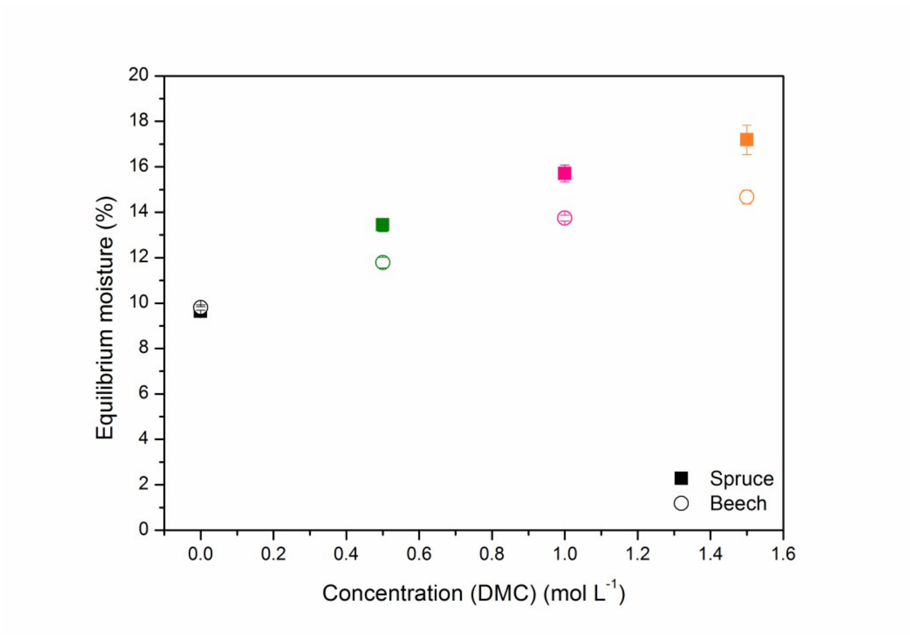

Figure S7. Equilibrium moisture of reference and mineralized wood as a function of the precursor concentration [DMC] = [$CaCl_2$] determined from the mass in the dry state (65° C) and at norm climate (65 % relative humidity, 20° C).

Thermogravimetric analysis

In addition to pyrolysis combustion flow calorimetry, thermogravimetric analysis gives complementary information on the mass loss in pure nitrogen at a constant heating rate. Below 100° C, the higher mass loss of the mineralized samples compared to the references (Figure S8-11) is attributed to their higher equilibrium moisture (see Figure S7). The first derivative allows to evaluate the slope of the TGA curve in the 100-500° C temperature range most relevant for wood combustion (Figure S9 and S11). Compared to the reference, the mineralisation treatment gives rise to a shift of the onset temperature to lower values and a decreased overall mass loss.

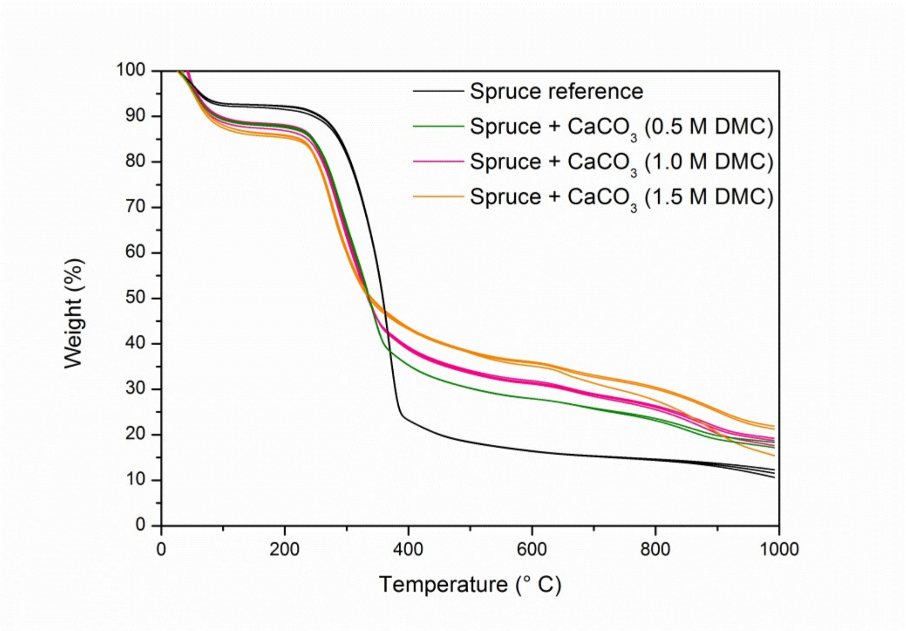

Figure S8. Thermogravimetric analysis of spruce composites in a temperature range 50-1000° C.

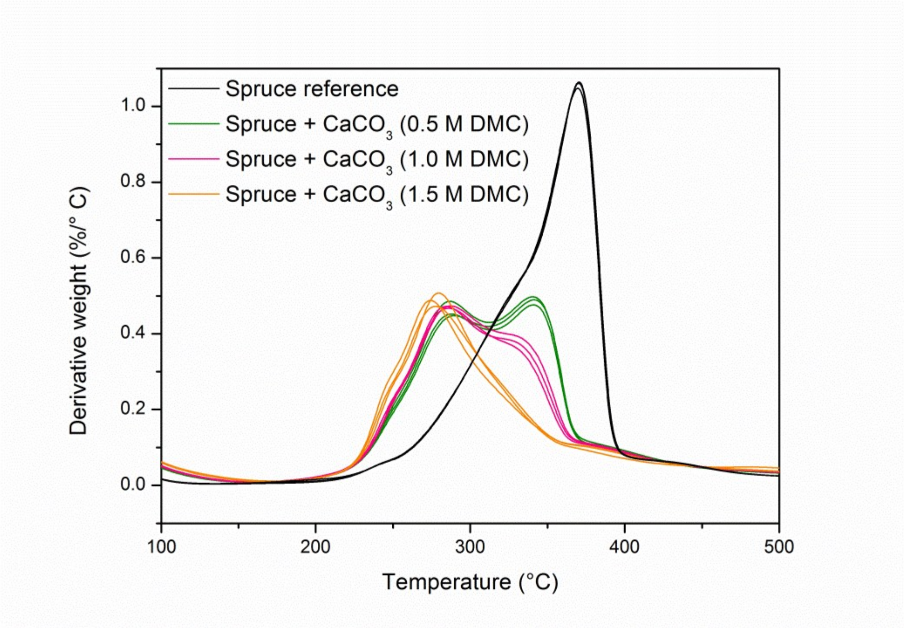

Figure S9. First derivative of thermogravimetrically determined mass of spruce composites in a temperature range 100-500° C.

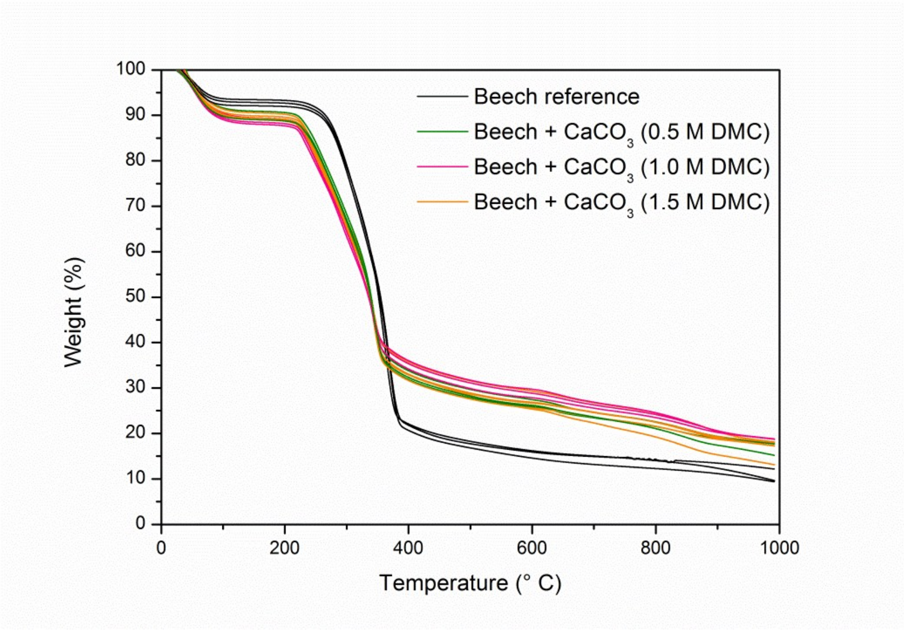

Figure S10. Thermogravimetric analysis of beech composites in a temperature range 50-1000° C.

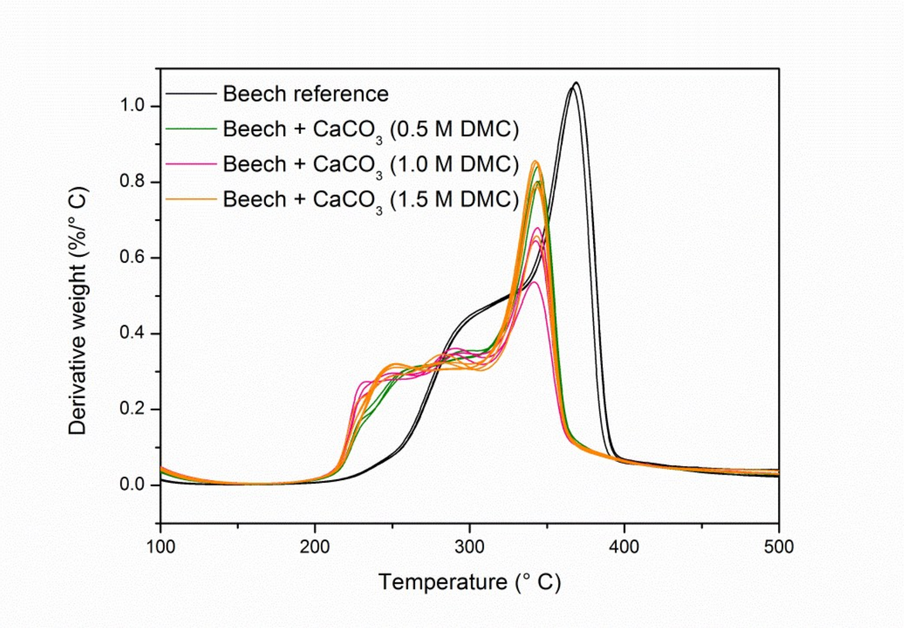

Figure S11. First derivative of thermogravimetrically determined mass of beech composites in a temperature range 100-500° C.

Scanning electron microscopy and semi-quantitative energy-dispersive X-ray analysis

Semi-quantitative energy-dispersive X-ray spectroscopy (SEM-EDX) of mineralized spruce and beech (precursor concentrations 1.5 M $CaCl_2$ and 1.5 M DMC) have been obtained in the center of an unwashed bulk specimen in 5 mm depth (Figure S12-15). It has to be taken into account that characteristic X-ray lines emerge from a bigger micron-ranged volume than the backscattered electrons in the SEM images. The relative elemental composition of the point analysis is given both in weight percentage (Wt%) and normalized atom percentage (At%). A comparison of the atom percentage of Na and Cl indicates that unreacted $CaCl_2$ is present apart from the reaction products NaCl and $CaCO_3$.

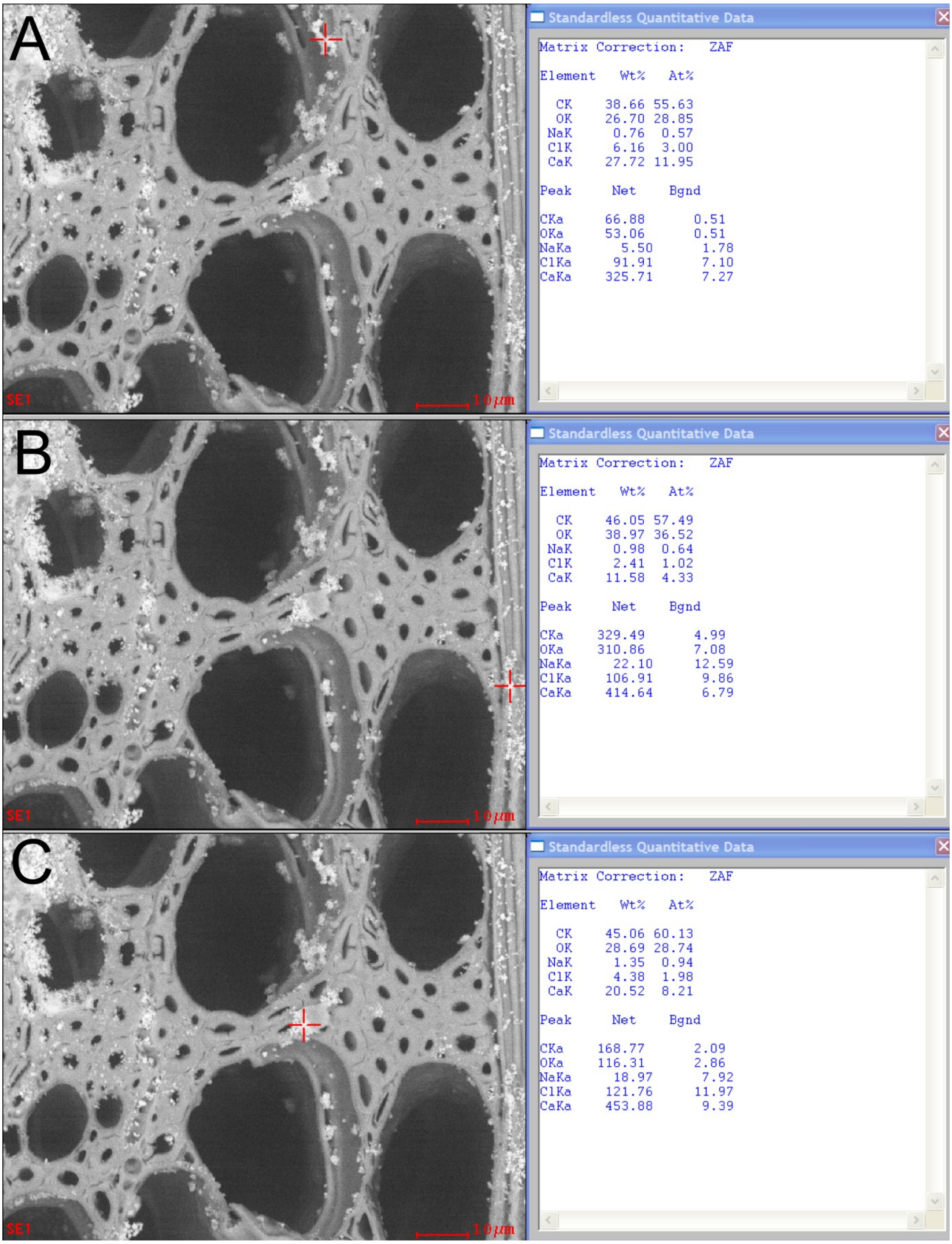

```
Matrix Correction:   ZAF

Element   Wt%   At%

  CK     38.66 55.63
  OK     26.70 28.85
 NaK      0.76  0.57
 ClK      6.16  3.00
 CaK     27.72 11.95

Peak      Net    Bgnd

CKa      66.88       0.51
OKa      53.06       0.51
NaKa       5.50       1.78
ClKa      91.91       7.10
CaKa     325.71       7.27
```

```
Matrix Correction:   ZAF

Element   Wt%   At%

  CK     46.05 57.49
  OK     38.97 36.52
 NaK      0.98  0.64
 ClK      2.41  1.02
 CaK     11.58  4.33

Peak      Net    Bgnd

CKa     329.49       4.99
OKa     310.86       7.08
NaKa      22.10      12.59
ClKa     106.91       9.86
CaKa     414.64       6.79
```

```
Matrix Correction:   ZAF

Element   Wt%   At%

  CK     45.06 60.13
  OK     28.69 28.74
 NaK      1.35  0.94
 ClK      4.38  1.98
 CaK     20.52  8.21

Peak      Net    Bgnd

CKa     168.77       2.09
OKa     116.31       2.86
NaKa      18.97       7.92
ClKa     121.76      11.97
CaKa     453.88       9.39
```

Figure S12A-C. SEM in the backscattered electron mode and semi-quantitative EDX analysis of $CaCO_3$/beech composites (non-washed, oven-dried at 65°C, conditioned to norm climate).

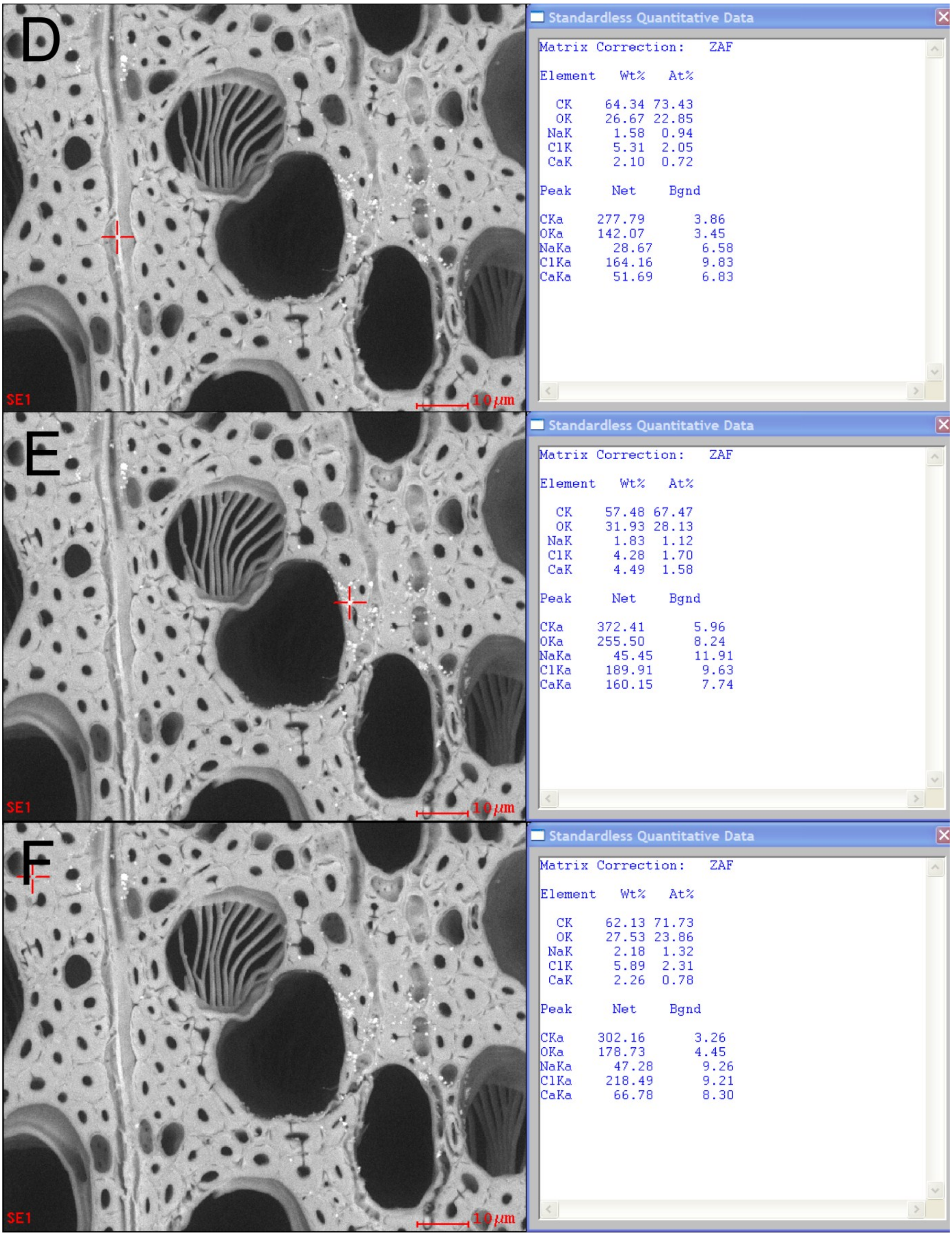

```
Matrix Correction:   ZAF

Element   Wt%   At%

  CK    64.34 73.43
  OK    26.67 22.85
 NaK     1.58  0.94
 ClK     5.31  2.05
 CaK     2.10  0.72

Peak      Net     Bgnd

CKa     277.79       3.86
OKa     142.07       3.45
NaKa     28.67        6.58
ClKa    164.16        9.83
CaKa     51.69        6.83
```

```
Matrix Correction:   ZAF

Element   Wt%   At%

  CK    57.48 67.47
  OK    31.93 28.13
 NaK     1.83  1.12
 ClK     4.28  1.70
 CaK     4.49  1.58

Peak      Net     Bgnd

CKa     372.41       5.96
OKa     255.50       8.24
NaKa     45.45       11.91
ClKa    189.91        9.63
CaKa    160.15        7.74
```

```
Matrix Correction:   ZAF

Element   Wt%   At%

  CK    62.13 71.73
  OK    27.53 23.86
 NaK     2.18  1.32
 ClK     5.89  2.31
 CaK     2.26  0.78

Peak      Net     Bgnd

CKa     302.16       3.26
OKa     178.73       4.45
NaKa     47.28        9.26
ClKa    218.49        9.21
CaKa     66.78        8.30
```

Figure S13D-F. SEM in the backscattered electron mode and semi-quantitative EDX analysis of $CaCO_3$/beech composites (non-washed, oven-dried at 65°C, conditioned to norm climate).

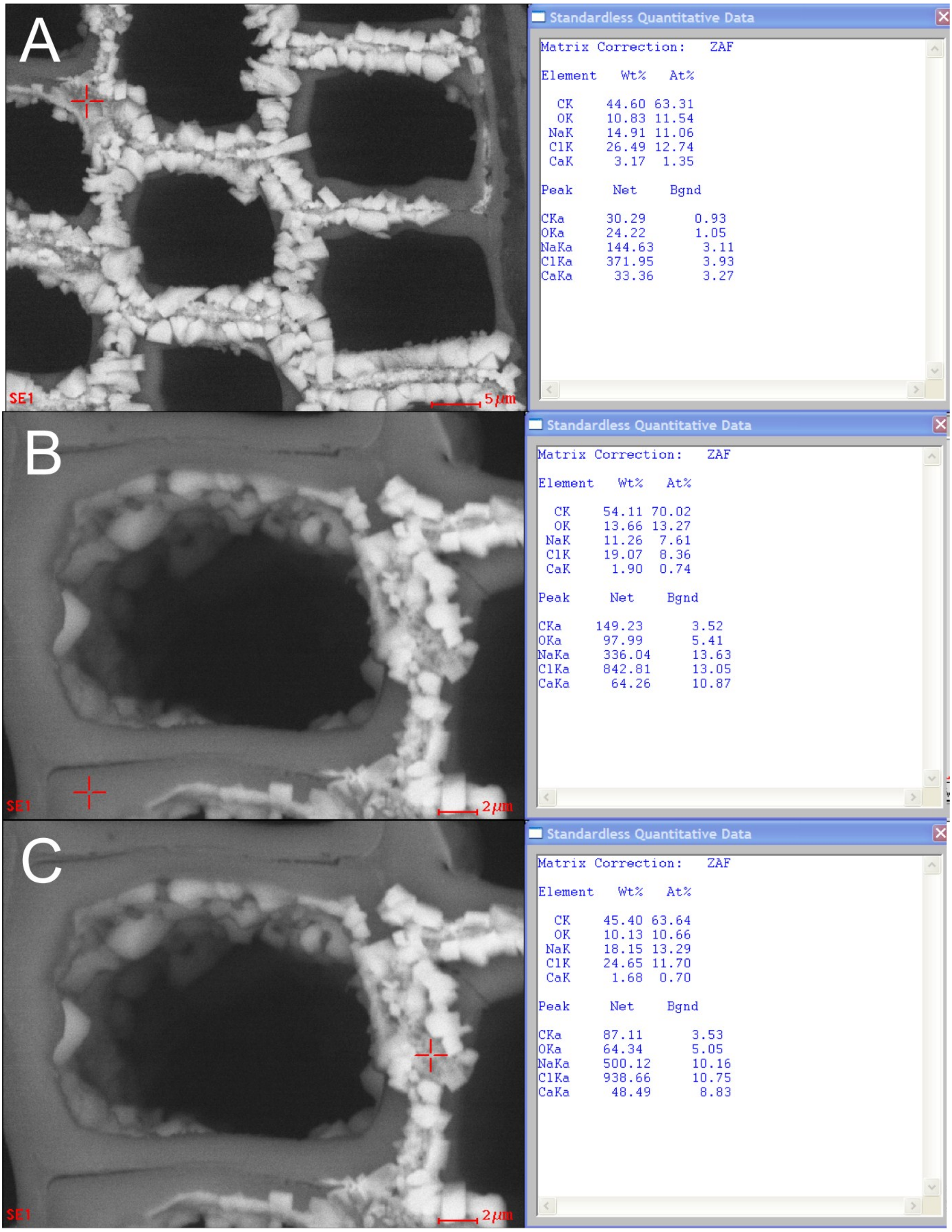

Standardless Quantitative Data

```
Matrix Correction:   ZAF

Element   Wt%   At%

  CK     44.60 63.31
  OK     10.83 11.54
 NaK     14.91 11.06
 ClK     26.49 12.74
 CaK      3.17  1.35

Peak      Net     Bgnd

CKa      30.29       0.93
OKa      24.22       1.05
NaKa     144.63       3.11
ClKa     371.95       3.93
CaKa      33.36       3.27
```

Standardless Quantitative Data

```
Matrix Correction:   ZAF

Element   Wt%   At%

  CK     54.11 70.02
  OK     13.66 13.27
 NaK     11.26  7.61
 ClK     19.07  8.36
 CaK      1.90  0.74

Peak      Net     Bgnd

CKa     149.23       3.52
OKa      97.99       5.41
NaKa    336.04      13.63
ClKa    842.81      13.05
CaKa     64.26      10.87
```

Standardless Quantitative Data

```
Matrix Correction:   ZAF

Element   Wt%   At%

  CK     45.40 63.64
  OK     10.13 10.66
 NaK     18.15 13.29
 ClK     24.65 11.70
 CaK      1.68  0.70

Peak      Net     Bgnd

CKa      87.11       3.53
OKa      64.34       5.05
NaKa    500.12      10.16
ClKa    938.66      10.75
CaKa     48.49       8.83
```

Figure S14A-C. SEM in the backscattered electron mode and semi-quantitative EDX analysis of $CaCO_3$/spruce composites (non-washed, oven-dried at 65°C, conditioned to norm climate).

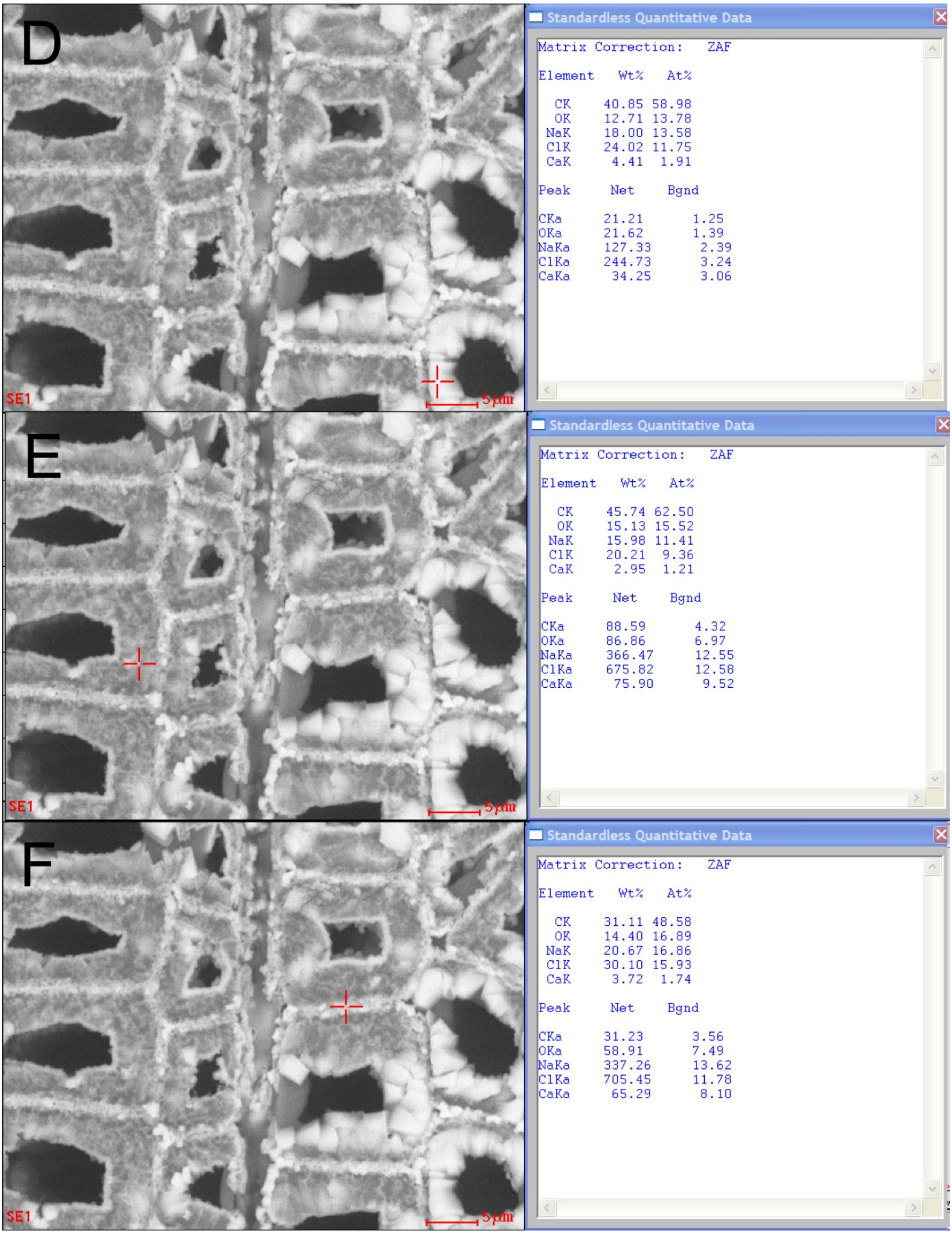

```
Matrix Correction:   ZAF

Element   Wt%   At%

  CK     40.85 58.98
  OK     12.71 13.78
 NaK     18.00 13.58
 ClK     24.02 11.75
 CaK      4.41  1.91

Peak      Net     Bgnd

CKa      21.21       1.25
OKa      21.62       1.39
NaKa     127.33       2.39
ClKa     244.73       3.24
CaKa      34.25       3.06
```

```
Matrix Correction:   ZAF

Element   Wt%   At%

  CK     45.74 62.50
  OK     15.13 15.52
 NaK     15.98 11.41
 ClK     20.21  9.36
 CaK      2.95  1.21

Peak      Net     Bgnd

CKa      88.59       4.32
OKa      86.86       6.97
NaKa     366.47      12.55
ClKa     675.82      12.58
CaKa      75.90       9.52
```

```
Matrix Correction:   ZAF

Element   Wt%   At%

  CK     31.11 48.58
  OK     14.40 16.89
 NaK     20.67 16.86
 ClK     30.10 15.93
 CaK      3.72  1.74

Peak      Net     Bgnd

CKa      31.23       3.56
OKa      58.91       7.49
NaKa     337.26      13.62
ClKa     705.45      11.78
CaKa      65.29       8.10
```

Figure S15D-F. SEM in the backscattered electron mode and semi-quantitative EDX analysis of $CaCO_3$/spruce composites (non-washed, oven-dried at 65°C, conditioned to norm climate).

X-ray powder diffraction

X-Ray powder diffraction of mineralized spruce without prior washing (Figure S16) demonstrates the formation of crystalline calcite ($CaCO_3$)[3] and sodium chloride (NaCl)[4] in the wood matrix, whereas the precursor salt calcium chloride dihydrate (sinjarite) is not detected in the XRD spectrum[5]. We calculated the XRD pattern from Q values of $CaCl_2 \cdot 2H_2O$ reported in the literature[5] for a copper X-ray source ($\lambda_{CuK\alpha}$ = 1.541838 Å) yielding 2Θ = 64.3°, 44.1°, 40.6°, 38.5°, 36.0°, 33.7°, 32.2°, 30.7°, 30.2°, 28.6°, 26.5°, 25.2°, 24.2°, 23.6°, 22.9°, 21.5°, 20.9°, given as dotted lines in Figure S16. After washing the mineralized spruce for 3 h in slightly basic water, sodium chloride is removed according to XRD (Figure S17). Nevertheless, the presence of amorphous $CaCO_3$ in the sample cannot be ruled out. Amorphous calcium carbonate gives rise to a broad peak around $2\Theta \approx 40°$ [6]. A quantification of amorphous mineral phases in wood tissues, however, is highly challenging due to a background from amorphous cellulose domains (Figure S18). A detailed characterization of mineralized wood using X-ray techniques will be a subject of future investigations.

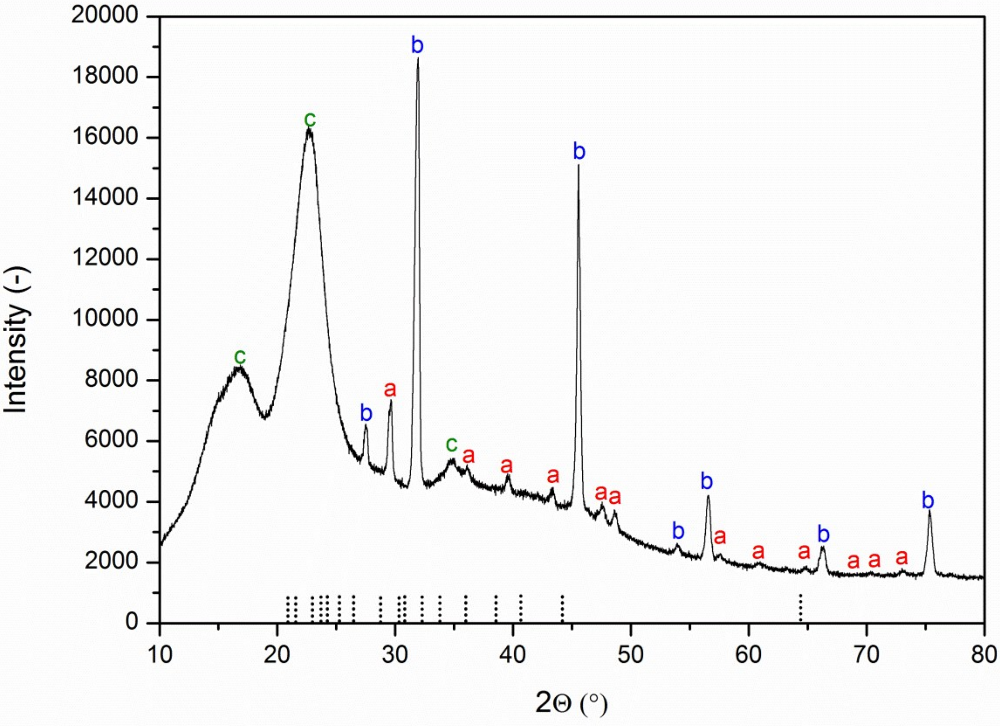

Figure S16. XRD of unwashed mineralized spruce showing crystalline portion of calcite (a), sodium chloride (b) and cellulose microfibrils (c). The dotted lines give the diffraction pattern of $CaCl_2 \cdot H_2O$ according to the literature[5].

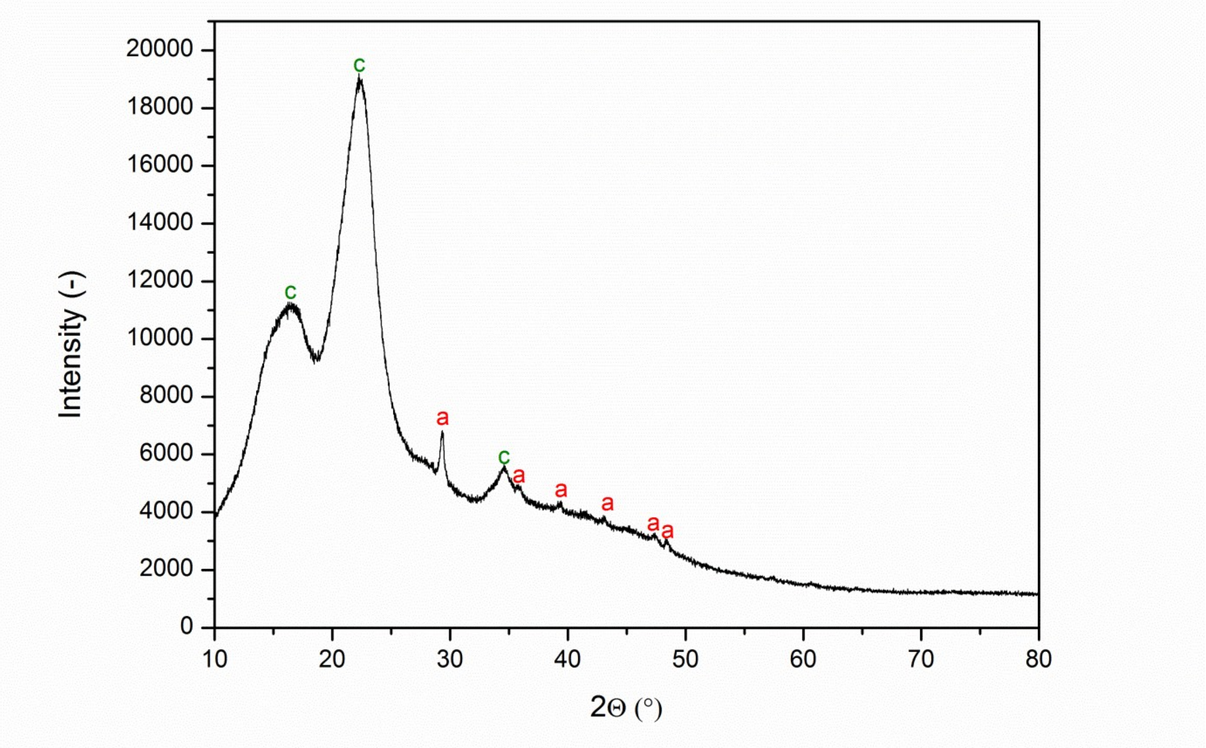

Figure S17. XRD of mineralized spruce washed in slightly basic water (pH ≈ 8) showing crystalline portion of calcite (a) and cellulose microfibrils (c).

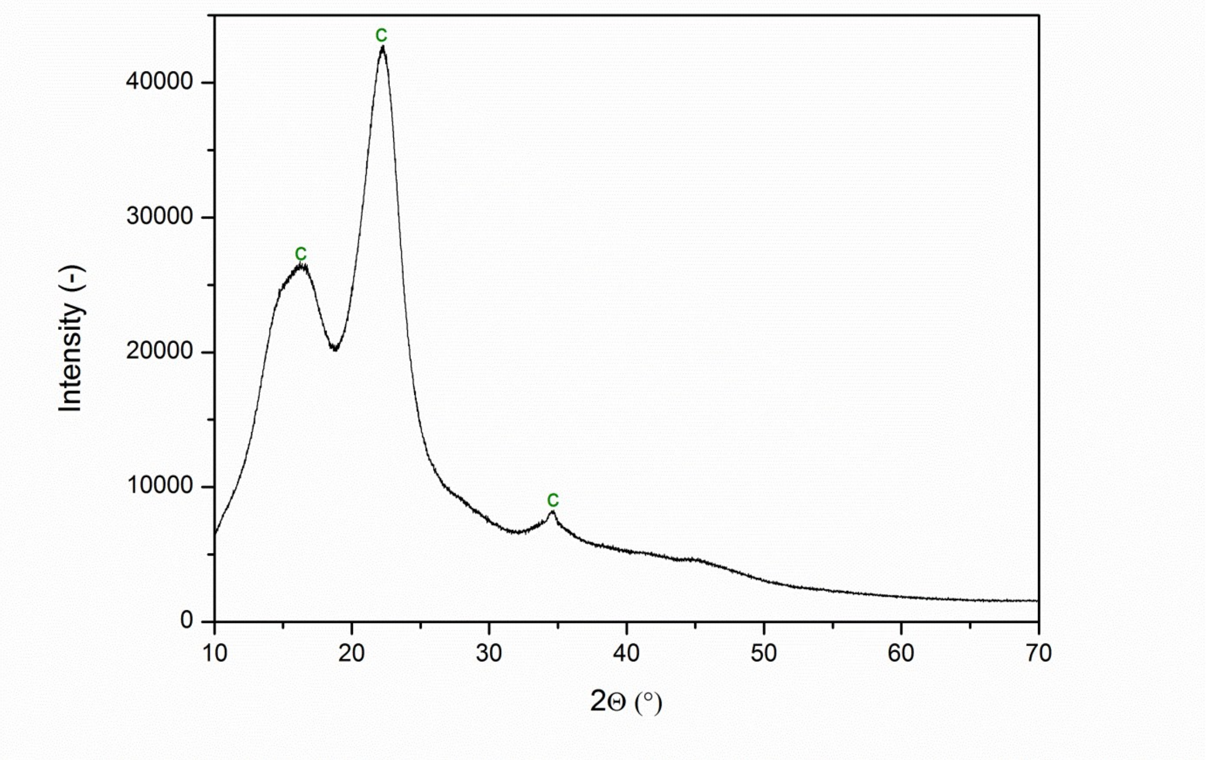

Figure S18. XRD of reference spruce showing cellulose microfibrils (c).

References

1. Lyon, R. E.; Walters, R. N., Pyrolysis combustion flow calorimetry. *Journal of Analytical and Applied Pyrolysis* **2004,** *71* (1), 27-46.
2. Andersen, F. A.; Brecevic, L., Infrared-spectra of amorphous and crystalline calcium carbonate. *Acta Chemica Scandinavica* **1991,** *45* (10), 1018-1024.
3. Kontoyannis, C. G.; Vagenas, N. V., Calcium carbonate phase analysis using XRD and FT-Raman spectroscopy. *Analyst* **2000,** *125* (2), 251-255.
4. Downs, R. T., The RRUFF Project: an integrated study of the chemistry, crystallography, Raman and infrared spectroscopy of minerals. In *Program and Abstracts of the 19th General Meeting of the International Mineralogical Association in Kobe*, Japan, **2006**; p Halite R070292.
5. Aljubouri, Z. A.; Aldabbagh, S. M., Sinjarite, a new mineral from Iraq. *Mineralogical Magazine* **1980,** *43* (329), 643-645.
6. Gorna, K.; Hund, M.; Vučak, M.; Gröhn, F.; Wegner, G., Amorphous calcium carbonate in form of spherical nanosized particles and its application as fillers for polymers. *Materials Science and Engineering: A* **2008,** *477* (1–2), 217-225.